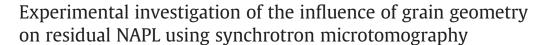
Contents lists available at ScienceDirect

Journal of Contaminant Hydrology

journal homepage: www.elsevier.com/locate/jconhyd



Riyadh I. Al-Raoush*

Department of Civil and Architectural Engineering, Qatar University, Doha, Qatar

ARTICLE INFO

Article history: Received 1 May 2013 Received in revised form 13 January 2014 Accepted 20 January 2014 Available online 2 February 2014

Keywords: Residual NAPL Microtomography Pore-scale Grain geometry Interfacial area

ABSTRACT

The objective of this work was to investigate the impact of grain geometry (size and shape) of porous media on the morphology of residual NAPL. Synchrotron microtomography was used to obtain maps of residual NAPL in multiphase systems. High-resolution, three-dimensional images of natural sand systems, comprising a range of grain sizes and shapes were imaged and analyzed. Findings indicate that residual NAPL saturation is influenced by the shapes of grains of the porous medium more than their sizes. In systems composed of grains swith similar sphericity and angularity, residual saturations are independent of median grain sizes at the same operating regime (capillary-controlled regime in this work). Residual saturations tend to increase as the system comprised more angular or non-spherical grains where relatively large NAPL blobs are entrapped in such systems. While volumes of individual blobs tend to decrease as grain size decreases, grain geometry has more profound effects on the morphology of the residual NAPL blobs. Within a system composed of grains with similar shape characteristics, total NAPL-water interfacial area increases as grain sizes decrease where a large number of small blobs are trapped.

Total meniscus NAPL–water interfacial area exhibits a linear relation with total interfacial area where it tends to increase as grain sizes decrease. However, while meniscus interfacial areas of individual blobs are highly influenced by pore geometry; residual blobs trapped in pores with complex geometry tend to have higher meniscus interfacial areas due to their branched nature which increases contacts with the wetting phase.

© 2014 Elsevier B.V. All rights reserved.

1. Introduction

Distribution, configuration and migration of nonaqueous phase liquids (NAPLs), such as gasoline and chlorinated solvents, in subsurface environments are of great importance for environmental and earth sciences research applications. The assessment, design and implementation of efficient cleanup and remediation strategies for systems containing residual NAPL are greatly influenced by pore-scale distribution, morphology and mass-transfer characteristics of the NAPL. Therefore, a thorough understanding of transport and mass transfer properties in porous materials and their dependence on pore geometry is critical.

* Tel.: +974 4403 4188; fax: +974 4403 4172. *E-mail address:* riyadh@qu.edu.qa.

In the past years, several investigations were conducted to characterize the morphology of NAPLs in porous media systems in order to gain a better understanding of pore-scale processes that govern macro-scale processes such as dissolution, pressure-saturation relations, and relative permeability. The main approaches used in these studies include direct observation of NAPLs in the pore space (Chatzis et al., 1983; Conrad et al., 1992; Mayer and Miller, 1992; Powers et al., 1992; Wardlaw and McKellar, 1985), two-dimensional etched-glass micromodels (Chomsurin and Werth, 2003; Jia et al., 1999; Sahloul et al., 2002) and three-dimensional imaging techniques (Al-Raoush and Willson, 2005a; Al-Raoush and Willson, 2005b; Culligan et al., 2004, 2006; Goldstein et al., 2007; Johns and Gladden, 1999, 2001; Schnaar and Brusseau, 2005; Zhang et al., 2002). While such investigations provide valuable insights about the characteristics of NAPL, the need to







^{0169-7722/\$ -} see front matter © 2014 Elsevier B.V. All rights reserved. http://dx.doi.org/10.1016/j.jconhyd.2014.01.008

obtain data that serve as benchmarks to improve our understanding of the physics of NAPL entrapment in porous media and to validate predictive pore-scale models is essential. This goal can be achieved by conducting well-designed, comprehensive experiments that incorporate well-characterized representative porous media. These well-controlled experiments allow acquisition of accurate three-dimensional maps of NAPL distributions and configurations under different experimental conditions. Data and findings obtained from these experiments can then be used to validate and improve physically based predictive pore-level models.

The objective of this work was to investigate the impact of grain geometry of porous media on the characteristics of residual NAPL. Synchrotron-based X-ray microtomography was used to obtain maps of residual NAPL in multiphase systems. High-resolution three-dimensional images of fourteen natural sand systems, comprising a range of grain sizes and shapes were imaged and analyzed. Robust three-dimensional image processing algorithms were used to compute NAPL morphology in these systems.

2. Materials and methods

2.1. Materials

Quartz and silica sands (Agsco Co., Wheeling, Illinois) of different sizes and shapes were used to model the porous media. Silica sand was selected to represent rounded geometry, whereas quartz sand was used to represent angular geometry. The range of grain sizes was selected to ensure that systems were representative by achieving the minimum representative elementary volume (REV) for porosity. Sand samples were sieved and thoroughly cleaned by distilled, deionized water several times and then oven-dried for 24 h. The sand was then cleaned by nitric acid, followed by several distilled, deionized water washes. Fourteen different porous media systems (not including replicas of each system) were prepared and investigated. Six systems of silica sand where the median grain

Table 1

Physical properties of the porous media used in the experiments.

diameter, D₅₀, ranged between 0.433 mm and 0.196 mm were investigated. To introduce the effect of angularity of grains in the investigation, six quartz systems and two mixed sand systems were included. The D₅₀ of quartz sand systems ranged between 0.431 mm and 0.179 mm. The mixed sands were created by mixing equal masses of silica and quartz sands. Note that the range of D₅₀ is narrow since the main focus is on the shape of grains. Physical properties of the porous media systems used in this investigation are given in Table 1. Immiscible fluids used in the experiments were de-aired water (the wetting phase) and Soltrol 220 (Chevron Philips Chemical Company) which was used to model NAPL (non-wetting phase). To obtain a distinguishable contrast between the phases in the images and thus, facilitate their segmentation, water was doped by CsCl (10% by weight) and Soltrol was doped by Iodobenzene (8% by volume). Furthermore, Soltrol was dyed by Oil Red O (Sigma-Aldrich Co.) to visually distinguish between the immiscible fluids and observe their flow. Previous investigations have shown that doping using agents and percentages used herein has a minimal impact on the properties of the immiscible fluids (Al-Raoush, 2009; Brusseau et al., 2007). The density and viscosity of the aqueous solution are 0.97 g/cm³ and 1.02 cP, respectively; and for the doped Soltrol, 0.78 g/cm³ and 4.79 cP, respectively. The interfacial tension between the dyed Soltrol and the aqueous solution was measured using a 21 du Nouy ring tensiometer (Fisher Scientific) and determined to be 39.4 dyn/cm. The sands are strongly water-wet systems. All experiments were conducted at room temperature (i.e., 23 °C).

2.2. Experimental method

A flow cell was manufactured to be mounted on the microtomography stage for imaging while flow of fluids was performed. The cell was made of an X-ray transparent thin aluminum column connected, at both ends, to stainless steel compression adaptors. The compression adaptor at the upper end of the column connected it to a syringe pump or to a drainage reservoir through flexible Teflon tubing. Direction of

Porous medium	Porosity	D ₅₀ (mm) ^a	$C_u^{\ b}$	C _c ^c	Ψ^{d}	X _v ^e
Silica sand: S1	0.347	0.433	1.858	1.146	0.914	0.835
Silica sand: S2	0.375	0.352	1.847	1.118	0.903	0.827
Silica sand: S3	0.338	0.271	1.793	1.059	0.890	0.815
Silica sand: S4	0.359	0.267	1.794	1.068	0.888	0.812
Silica sand: S5	0.325	0.258	1.831	1.004	0.890	0.815
Silica sand: S6	0.383	0.196	1.524	1.086	0.883	0.807
Quartz sand: Q1	0.457	0.431	1.443	0.939	0.809	0.715
Quartz sand: Q2	0.455	0.276	2.494	1.062	0.815	0.725
Quartz sand: Q3	0.451	0.237	1.953	1.074	0.818	0.714
Quartz sand: Q4	0.450	0.233	2.144	1.076	0.813	0.725
Quartz sand: Q5	0.458	0.213	1.976	1.006	0.825	0.738
Quartz sand: Q6	0.456	0.179	1.720	1.059	0.813	0.727
Mixed: M1 50%S2 + 50%Q2	0.409	0.298	2.461	1.064	0.842	0.757
Mixed: M1 50%S3 + 50%Q3	0.420	0.252	1.959	1.094	0.852	0.772

^a D₅₀: Median grain diameter.

^b C_u : Uniformity coefficient = D_{60} / D_{10} .

^c C_c: Coefficient of gradation = $D_{30}^2 / (D_{60} * D_{10})$.

d Sphericity index.

e Roundness index.

Download English Version:

https://daneshyari.com/en/article/4546600

Download Persian Version:

https://daneshyari.com/article/4546600

Daneshyari.com